



Published in final edited form as:

Int J Cancer. 2017 October 15; 141(8): 1589–1599. doi:10.1002/ijc.30851.

Development of *Kras* mutant lung adenocarcinoma in mice with knockout of the airway lineage-specific gene *Gprc5a*

Junya Fujimoto^{1,*}, Sayuri Nunomura-Nakamura^{1,2,*}, Yihua Liu³, Wenhua Lang¹, Tina McDowell¹, Yasminka Jakubek³, Dalia Ezzeddine⁴, Joshua Kapere Ochieng¹, Jason Petersen⁵, Gareth Davies⁵, Junya Fukuoka², Ignacio I. Wistuba¹, Erik Ehl⁵, Jerry Fowler³, Paul Scheet^{3,‡}, and Humam Kadara^{1,6,‡}

¹Department of Translational Molecular Pathology, The University of Texas MD Anderson Cancer Center, Houston, TX, USA

²Graduate School of Biomedical Science, Nagasaki University, Nagasaki, Japan

³Department of Epidemiology, The University of Texas MD Anderson Cancer Center, Houston, TX, USA

⁴Department of Chemistry, American University of Beirut, Beirut, Lebanon

⁵Avera Institute for Human Genetics, Sioux Falls, SD, USA

⁶Department of Biochemistry and Molecular Genetics, Faculty of Medicine, American University of Beirut, Beirut, Lebanon

Abstract

Despite the urgency for prevention and treatment of lung adenocarcinoma (LUAD), we still do not know drivers in pathogenesis of the disease. Earlier work revealed that mice with knockout of the G-protein coupled receptor *Gprc5a* develop late onset lung tumors including LUADs. Here, we sought to further probe the impact of *Gprc5a* expression on LUAD pathogenesis. We first surveyed *GPRC5A* expression in human tissues and found that *GPRC5A* was markedly elevated in human normal lung relative to other normal tissues and was consistently down-regulated in LUADs. In sharp contrast to wild type littermates, *Gprc5a*^{-/-} mice treated chronically with the nicotine-specific carcinogen NNK developed LUADs by six months following NNK exposure.

Immunofluorescence analysis revealed that the LUADs exhibited abundant expression of surfactant protein C and lacked the clara cell marker *Ccsp*, suggesting that these LUADs originated from alveolar type II cells. Next, we sought to survey genome-wide alterations in the pathogenesis of *Gprc5a*^{-/-} LUADs. Using whole exome sequencing, we found that carcinogen-induced LUADs exhibited markedly higher somatic mutation burdens relative to spontaneous tumors. All LUADs were found to harbor somatic mutations in the *Kras* oncogene (p. G12D or p.

Correspondence: Paul Scheet, Ph.D., Department of Epidemiology, The University of Texas MD Anderson Cancer Center, Houston, TX, 77030, USA, Telephone: 713-745-2470, pscheet@alum.wustl.edu or Humam Kadara, Ph.D., Department of Biochemistry and Molecular Genetics, Faculty of Medicine, American University of Beirut, Beirut, Lebanon, Telephone: +9611350000, Fax:

+9611744464, hk94@aub.edu.lb.

*Equally contributing co-first authors

‡Equally contributing co-corresponding authors

The authors report no conflicts of interests.

Q61R). In contrast to spontaneous lesions, carcinogen-induced *Gprc5a*^{-/-} LUADs exhibited mutations (variants and copy number gain) in additional drivers (*Atm*, *Kmt2d*, *Nf1*, *Trp53*, *Met*, *Ezh2*). Our study underscores genomic alterations that represent early events in the development of *Kras* mutant LUAD following *Gprc5a* loss and tobacco carcinogen exposure and that may constitute targets for prevention and early treatment of this disease.

Keywords

Lung adenocarcinoma; carcinogenesis; *Gprc5a*; *Kras*; whole-exome sequencing

Introduction

Non-small cell lung cancer (NSCLC) is the leading cause of cancer-deaths in the United States and worldwide ^{1,2}. The majority (~85%) of diagnosed NSCLC cases are attributed to cigarette smoking (tobacco carcinogen exposure) ^{3,4}. Lung adenocarcinoma (LUAD) represents the most commonly diagnosed histological subtype of NSCLC in former or current smokers ^{3,4}. While smoking cessation has been shown to reduce the risk of developing LUAD, this risk does not return to a baseline level for former smokers ^{5,6}. Various mutational profiling studies have revealed disparate molecular subtypes of LUAD ⁷⁻¹⁰ that are closely associated with tobacco consumption history. While somatic activating mutations in the epidermal growth factor receptor (*EGFR*) oncogene are prevalent in LUADs that develop in non-smokers, mutations in the Kirsten rat sarcoma oncogene (*KRAS*) are prevalent in smoker LUADs ^{3,7-11}. Particular molecular subtypes of LUAD (e.g. *KRAS* mutant LUADs) display dismal clinical outcomes and are resistant to various forms of targeted therapies ^{12,13} thus warranting the need for new strategies for early treatment of this malignancy.

Earlier studies have underscored restricted patterns of gene expression in lung epithelial and malignant cells ⁴. For instance, the embryonic stem cell transcription factor, sry-box 2 (*SOX2*) is preferentially found in the conducting airway epithelia ¹⁴, the presumed cell-of-origin of squamous NSCLCs ¹⁵. *SOX2* promotes growth of squamous NSCLC cells and has been shown to be specifically up-regulated in squamous NSCLC ^{14,16,17}. The transcription factor NK2 homeobox 1 (*NKX2-1* also known as *TTF-1*) is prevalent in peripheral lung cells (alveolar cells) ¹⁸, the presumed anatomical origin of LUADs ¹⁵. *NKX2-1* was demonstrated to be preferentially gained in a significant fraction of LUADs but not in squamous NSCLCs ^{7,19}, and to function as a lineage-specific oncogene in LUADs ²⁰. The retinoid-inducible G-protein coupled receptor, *Gprc5a*, was shown to be preferentially expressed in fetal and adult normal lung ²¹. Mice with knockout of both alleles of *Gprc5a* (*Gprc5a*^{-/-}) in the presence or absence of mild exposure (single dose) to the nicotine-specific nitrosamine ketone (NNK) tobacco carcinogen, and in sharp contrast to similarly treated wild type (WT) littermates, develop latent LUADs ^{22,23}. While these earlier reports suggest that *Gprc5a* may function as a lung lineage-specific tumor suppressor, the molecular pathogenesis of LUADs, including those linked to smoking, following *Gprc5a* knockout remains elusive.

Our present study was aimed at furthering our understanding of the impact of *Gprc5a* expression on LUAD pathogenesis. We demonstrate that human *GPRC5A* is largely preferentially expressed in normal lung epithelia relative to other normal tissues, is down-regulated in smoking-exposed normal-appearing airway cells and is consistently suppressed in LUADs. Following *in vivo* carcinogenesis analyses, we find that chronic exposure of *Gprc5a*^{-/-} mice to NNK, in contrast to saline-treated mice with latent tumor development, results in accelerated malignant adenocarcinoma onset within 6 months after exposure. Surveying genome-wide alterations in *Gprc5a*^{-/-} LUADs by whole-exome sequencing, we report somatic activating mutations in the *Kras* oncogene in both spontaneous and NNK-associated LUADs. In contrast to spontaneous tumors, carcinogen-induced *Gprc5a*^{-/-} LUADs exhibited mutations and copy number alterations in additional drivers. Our study highlights genomic aberrations in the early progression of *Kras* mutant LUAD following *Gprc5a* knockout and tobacco carcinogen exposure. These aberrations may comprise viable targets for prevention and treatment of this aggressive molecular subtype of LUAD.

Materials And Methods

Chemical and reagents

The tobacco carcinogen NNK with a purity of greater than 99% was purchased from Midwest Research Institute (The National Cancer Institute's Chemical Carcinogen Reference Standard Repository). Hematoxylin and Eosin (H&E) staining reagents were purchased from Sigma-Aldrich.

Animal housing and tobacco carcinogen experiments

We used *Gprc5a* knockout (*Gprc5a*^{-/-}) mice, which were generated as described previously²³. The mice were maintained according to a protocol approved by the MD Anderson Cancer Center Institutional Animal Care and Use Committee at the institution's specific pathogen-free animal facility. This facility is approved by the American Association for Accreditation of Laboratory Animal Care and is operated in accordance with current regulations and standards of the US Department of Agriculture and the Department of Health and Human Services. *Gprc5a*^{-/-} (2 months old) were divided into groups (per treatment and sacrifice time point) of 5 or 6 mice and were injected three times per week (for eight weeks) intraperitoneally with 50 mg/kg of body weight NNK (150 mg/kg per week) dissolved in saline or with saline alone as control. Mice were sacrificed at every month for seven months following NNK or saline injection. A subset of mice exposed to control saline were sacrificed at later time points (> 16 months following saline) to capture late onset spontaneous lung adenocarcinomas.

Histopathological analysis of lung lesions

After sacrifice at different time points, lungs were excised and inflated by injection with formalin for lesion histopathological assessment. Lung surface lesions were assessed by macroscopic observation. Formalin-fixed lung specimens were then embedded in paraffin (FFPE). Histological sections (four μm) were prepared and analyzed by H&E staining using standardized criteria²⁴ for characterization and diagnosis of lung lesions (hyperplasias, adenomas and adenocarcinomas) by an experienced pathologist (J.F.). Lesions were

enumerated from each slide/section to yield a tumor burden per lung specimen. All H&E slides were scanned by Aperio (Leica biosystems Inc.).

Immunofluorescence (IF) analysis

Lungs were injected with a mixture of 50% optimal cutting temperature (OCT) medium (Tissue-Tek) and 50% PBS. Frozen histologic sections (5 μ m thick) from adult mice were fixed in ice-cold 4% buffered paraformaldehyde for 15 min. Embryos (day 16.5) from WT mice were cut and immersed in 10% buffered formalin (two days) for subsequent IF analysis. After washing, sections were first incubated with serum-free protein block (DAKO) for 1 hour. Specimens were then incubated with antibodies raised against clara cell secretory protein (Ccsp/CC10; Santa Cruz Biotechnology; 1:250) and prosurfactant protein C (Sftpc; Chemicon EMD Millipore, 1:200) overnight. After washing, specimens were incubated with FITC-labeled donkey anti-goat secondary antibody (Alexa 488) for 1.5 h in the dark followed by washing and incubation with Texas Red-labeled goat-anti-rabbit secondary antibody (Alexa 594). Slides were then incubated with ProLong® Gold Antifade Reagent with DAPI (Cell Signaling Technology). To assess Gprc5a expression, specimens were incubated after blocking with a mixture of antibodies raised against Gprc5a (Santa Cruz Biotechnology; 1:25), Podoplanin (Pdpn; DSHB; 1:400 dilution) and Sftpc (1:10). The specimens were then washed and incubated with FITC-labeled donkey anti-goat secondary antibody (Alexa 488) and Texas Red-labeled goat anti-rabbit secondary antibody (Alexa 594) or with Texas Red-labeled donkey anti-goat secondary antibody (Alexa 594) and FITC-labeled goat anti-rabbit secondary antibody (Alexa 488) for 1.5 h in the dark. All images were captured using a BX61 immunofluorescent system (Olympus) and merged using the CytoVision workstation (Leica biosystems Inc.) at magnification of 200 \times .

DNA isolation and quality control

Genomic DNA was isolated from lung lesions using 50 μ m FFPE sections prepared by the Bio-bank system (Pathology Institute Corp., Toyama, Japan). Genomic DNA was isolated from all samples using the AllPrep DNA/RNA kit from Qiagen according to the manufacturer's instructions. Quality of double-stranded DNA was ascertained using the Picogreen kit according to the manufacturer's instructions.

Whole-exome sequencing (WES)

Sequencing was performed on seven LUADs from different mice (two spontaneous occurring LUADs at 16 months following saline and five LUADs at 5-7 months following NNK exposure; Supplementary Table 1). We also sequenced three tail veins from one wild type and two *Gprc5a*^{-/-} mice as well as *Gprc5a*^{-/-} normal lung tissues at one month following saline or NNK for somatic contrasts in the manner described previously²⁵. DNA libraries, using 200-500 ng of qualified DNA, for massively parallel sequencing were prepared using the SureSelect^{XT} Target Enrichment System for according to the manufacturer's instructions (Agilent Technologies). Library quality and quantity were assessed using a DNA 1000 chip on a 2100 Bioanalyzer. Library fragments were hybridized to the SureSelect^{XT} Mouse All Exon Capture Library (49.6 MB capture) according the manufacturer's protocol. Paired-end cluster generation of denatured templates was performed according to the manufacturer's instructions (Illumina, San Diego, CA) using the HiSeq PE Cluster Kit v4 chemistry and

flow cells. WES was performed using the Illumina HiSeq 2500 platform (Illumina, San Diego, CA) utilizing v4 chemistry with paired-end 101 bp reads. Illumina BaseSpace FastQ v1.0.0 was used to de-multiplex and convert the .bcl files to FastQ files for downstream analyses. An average of 196 million unique on-target sequence reads per sample were produced (Table S1).

Identification of somatic variants and copy number variation

Alignment was performed according to Genome Analysis Toolkit (GATK) best practices using burrows-wheeler aligner (BWA) version 0.6.2, GATK-2.6-4, picard-1.114, and samtools-0.1.19 against the mm10 reference with realignments performed using the mouse indel reference mmp.v3.indels.rsIDdbSNPv137. Exomes were filtered against the Agilent M.musculus-SureSelect.Exon.V1.mm10.bed.intervals file corresponding to the capture technology. Somatic variation detection was performed using MuTect-1.1.7 and IndelGenotyper.36.3336 against the same references Annotations were made using variant_tools-2.6.1, using the same references as well as the mouse snp reference mmp.v3.snps.rsIDdbSNPv137. Variants were further filtered for known variants from the database of mouse variation available at ftp-mouse.sanger.ac.uk (release 1303, mmp.v3) ²⁵. Given the scarcity of recurrent variants in the dataset, (thus preventing us from prioritizing genes by adjusting for gene expression and replication timing ²⁶, variants were prioritized for those that occurred in genes described by Vogelstein and colleagues ²⁷ as known to contain *bona fide* driver mutations in cancer. Mutations in *Trp53* as well as in *Mtus1* were also prioritized based on the report by Westcott and colleagues ²⁵. Gene homology information between human and mouse genes were obtained from <ftp://ftp.informatics.jax.org/pub/reports/index.html#homology>. To compute copy number variations (CNVs) from the sequencing data, the control-FREEC algorithm version 7.2 was employed using run settings described previously ²⁸ as well as Sequenza (version 0.0.3) ²⁹. The CNVs were called through tumor-normal comparisons where each LUAD was compared to the normal lung tissues and tail veins.

More details are found in the Supplementary Methods accompanying the manuscript.

Results

Lung lineage-specific tumor suppressor expression patterns for human *GPRC5A*

The G-protein coupled receptor, *Gprc5a*, has been previously shown to be preferentially expressed in mouse fetal and adult lung ²¹. Moreover, mice with knockout of both alleles of this gene (*Gprc5a*^{-/-}) in the presence or absence of low-dose tobacco carcinogen (single injection of nicotine-specific nitrosamine ketone/NNK), in sharp contrast to wild type littermates, have been demonstrated to develop late onset lung tumors, including LUADs ^{22, 23}, suggesting a tumor suppressor role for this gene in the lung. In the present study, we aimed to better understand the impact of *Gprc5a* expression on LUAD pathogenesis. We first sought to understand the expression patterns of the human counterpart of the gene (*GPRC5A*) in normal and malignant human lung tissues. We surveyed a publicly available dataset comprised of human normal tissues from various organs (pan-normal specimens; see Supplementary Methods). This analysis demonstrated that *GPRC5A* was highly expressed in

lung tissues (lung, trachea, bronchus) relative to other organ-specific normal tissues (Figure 1A). Next we probed publicly available datasets comprised of LUADs and uninvolved normal lung tissues (see Supplementary Methods). *GPRC5A* levels were markedly significantly, and consistently, down-regulated in LUADs compared to normal lung tissues in all datasets tested (all $P < 10^{-3}$; Figure 1B). We then sought to understand the association between *GPRC5A* expression and LUAD histopathological subtype. Towards this, we evaluated a tissue microarray of LUADs that we previously studied for *GPRC5A* immunohistochemical protein expression³⁰. This analysis revealed no significant differences in *GPRC5A* protein expression between lepidic, acinar, solid and papillary LUADs ($P = 0.29$ of the Kruskal-Wallis test; Figure S1). Next we determined to understand expression patterns of *GPRC5A* in early phases (e.g. “normal-appearing airway field cancerization (ref Kadara)” or “pre-malignant”) of LUAD pathogenesis. We performed *in silico* analysis of a dataset we recently reported on the tumor-adjacent cancerization field in the normal-appearing airway³¹, and found that *GPRC5A* was significantly suppressed in both LUADs and adjacent normal-appearing airway cells relative to distant normal lung ($P < 10^{-4}$; Figure S1). These data suggest plausible airway-lineage expression patterns and properties for *GPRC5A* in normal and malignant lung epithelial cells.

LUAD development following tobacco carcinogen exposure in *Gprc5a*^{-/-} mice

As mentioned earlier, we found that single dose (104 mg/kg body weight) of NNK lead to development of late onset spontaneous LUADs in *Gprc5a*^{-/-} mice²². We determined to perform a relatively more chronic NNK exposure in *Gprc5a*^{-/-} mice in an attempt to better emulate tobacco carcinogen-associated LUAD development. *Gprc5a*^{-/-} mice were divided into groups of five to six mice (per treatment and time point) and were injected intraperitoneally three times per week (for eight weeks) with 50 mg/kg of body weight NNK (150 mg/kg per week) dissolved in saline (0.9% NaCl) or with saline alone as control (Figure 2A). Mice were then sacrificed at each month for seven months after saline or NNK treatment (Figure 2A). Histopathological analysis was performed at each time point to probe the development of hyperplasias, adenomas and adenocarcinomas (Figure S3) based on previously reported criteria for classification of proliferative mouse lung lesions²⁴ including presence of nuclear atypia in adenocarcinoma tumors (Figure S3). In sharp contrast to mice treated with saline, NNK-treated *Gprc5a*^{-/-} mice developed LUADs as early as 3 months following NNK exposure (Figure 2B). Moreover, by six months following NNK, all (100%) *Gprc5a*^{-/-} mice were found to develop LUADs. Of note, saline treated *Gprc5a*^{-/-} mice did not exhibit LUADs across all time points but rather displayed lung adenomas or hyperplasias (Figure 2B, Figure S3). Of note, we also found significantly ($P < 0.05$) increased numbers of LUADs per mouse at seven relative to six months following NNK treatment (Figure 2C). A subset of saline treated mice were followed up for extended periods and were sacrificed at the time of spontaneous/latent LUAD development (see Materials and Methods). None of the mice developed locoregional or distant metastasis, an observation similar to what was previously reported for mice engineered to express mutant *Kras*³².

Next we sought to understand the airway lineage cell-of-origin of LUADs in the NNK-treated *Gprc5a*^{-/-} mice. We performed immunofluorescence (IF) analysis of lesions and adjacent normal bronchi probing for the expression of prototypical markers of airway

lineages including surfactant protein C (*Sftpc*), indicative of alveolar type II (AT2) cells, and clara cell secretory protein (*Ccsp/Cc10*), indicative of clara/club cells. In contrast to normal bronchial regions, lung lesions were found to lack *Ccsp* and abundantly express *Sftpc* suggesting that the cells of origin for these lesions were AT2 cells. Of note, IF analysis of normal wild type (WT) adult (Figure 3B) and embryonic (Figure S4) lung tissue as well as quantitative-real time PCR of CD45-/CD31-/Epcam+ WT normal lung cells sorted based on Podoplanin (*Pdpn*) expression (Figure S5) revealed that *Gprc5a* itself was restricted to *Pdpn*-expressing AT1 cells. Our findings demonstrate that tobacco carcinogen (NNK) exposure accelerates *Gprc5a*^{-/-} LUAD development, and suggest that these lesions originate from AT2 cells.

Mutational landscape of tobacco carcinogen exposed *Gprc5a*^{-/-} LUADs

We then sought to understand genome-wide alterations in the pathogenesis of the LUADs in tobacco carcinogen exposed *Gprc5a*^{-/-} mice. Using the Illumina HiSeq 2500 platform, we performed WES of seven *Gprc5a*^{-/-} LUADs; two spontaneously developing LUADs from two saline treated mice (>16 months after saline) and five tumors (from five mice) that developed five to seven months after NNK treatment. In accordance with previously reported criteria on classification of proliferative mouse lung lesions²⁴, all seven LUADs were confirmed to have either nuclear atypia (Figure S6; white arrows) or both nuclear atypia and evidence of cellular mitosis (Figure S6; red arrows). We then inferred somatic contrasts, in the manner described previously²⁵, by also sequencing three tail veins from one WT and two *Gprc5a*^{-/-} mice as well as two *Gprc5a*^{-/-} normal lung tissues at one month following saline or NNK. Targeted bases were sequenced to a mean depth of 215× (Table S1). Across samples, 99%, 97% and 86% of targeted bases were sequenced to at least 10×, 20× and 50× coverage, respectively (Table S1). There were no significant differences in depth of coverage or proportion of regions covered to 20× among samples (Table S1). In these seven LUADs, we identified 5,223 exonic single nucleotide variants (SNVs). Of note, LUADs that developed in NNK-exposed *Gprc5a*^{-/-} mice exhibited substantially higher mutation burdens (Figure S7, left) and different base substitution spectra (Figure S7, right) compared with spontaneously developing tumors, consistent with what is known about smoking-induced human LUADs^{3, 7, 8, 10}.

Next we sought to discern potential somatic driver mutations in the LUADs by prioritization of exonic and nonsynonymous variants. We compiled exonic nonsynonymous variants that occurred in genes described by Vogelstein and colleagues²⁷ as known to contain *bona fide* driver mutations in cancer (see Supplementary Methods). We also included mutations in *Trp53* as well as in *Mtus1* based on the report by Westcott and colleagues²⁵. Notably, this analysis revealed that all LUADs exhibited somatic activating mutations in *Kras* (p.G12D or P.Q61R) (Figure 4, Table S2), the same variants purported to act as drivers of human LUAD in smokers^{3, 11}. We also confirmed these *Kras* p.G12D and p.Q61R mutations by deep (> 1,000×) targeted sequencing (Ion Torrent) and digital PCR; both platforms revealed similar variant allele frequencies (VAFs) for the SNVs (Figures S8A-D). The NNK-exposed LUADs exhibited additional *driver* genes that were mutated in at least one LUAD including the cell cycle kinase *Atm* and the epigenetic modulator and methyltransferase *Kmt2d* as well as the tumor suppressors *Apc*, *Nf1* and *Trp53* (Figure 4), of which a subset was confirmed by deep

targeted sequencing (> 1,000×) (Figure S9). The spontaneous LUADs, albeit few, exhibited very few mutated driver genes besides *Kras*. Of note, one NNK-exposed LUAD, unlike the other four similar carcinogen derived tumors, exhibited a low somatic mutational burden concomitant with a mutation in p.Q61R (Figure 4). Of note, we found no significant differences in *GPRC5A* expression among human LUADs based on the type of *KRAS* codon 12 variant (Figure S10A) or between *KRAS*-mutant LUADs with and without *TP53* mutations (Figure S10B). We next surveyed genome-wide copy number variations (CNVs) in the seven LUADs (see Materials and Methods) and found disparate global CNV patterns between NNK-exposed and spontaneous *Gprc5a*^{-/-} LUADs (Figure 5). Four out of the five NNK-exposed LUADs, which we had found to exhibit high mutational burdens and specifically a p.G12D *Kras* mutation, shared gains in broad regions within chromosome 6 (Figure 5). These shared CNVs, along with other copy number gains not found in spontaneous LUAD, included the oncogenes *Kras*, *Met*, *Braf* and *Ezh2*. Our findings highlight genomic alterations that may play crucial roles in accelerated development and progression of *Kras* mutant LUADs in presence of tobacco carcinogen exposure.

Discussion

In this study we sought to further understand the role of *Gprc5a* expression in LUAD pathogenesis. First we surveyed publicly available expression datasets and found that human *GPRC5A* was largely preferentially expressed in normal lung tissues relative to other organ-specific normal samples and was also consistently suppressed in LUADs. We found that *Gprc5a*^{-/-} mice exposed to a relatively chronic NNK treatment regimen resulted in development of LUADs (within 5 months after exposure) as opposed to the latent development (> 16 months following saline treatment) in control treated mice. Whole-exome sequencing of latent (from saline treated mice) and NNK-associated *Gprc5a*^{-/-} LUADs, revealed activating somatic activating *Kras* mutations in all tumors. Additional (besides *Kras*) driver mutations and copy number alterations were also found in NNK-associated (and not in latent) *Gprc5a*^{-/-} LUADs that may underlie the observed accelerated *Kras* mutant LUAD development by tobacco carcinogen exposure. Our findings pinpoint genome-wide alterations that may be implicated in the progression of *Kras* mutant LUADs (by smoking).

The G-protein coupled receptor, *Gprc5a*, is a retinoid-inducible gene that was shown to be specifically expressed in murine normal lung tissues²¹. *Gprc5a*^{-/-} mice were demonstrated to develop late onset LUADs spontaneously^{22, 23}, suggesting that *Gprc5a* may function as a lung lineage-specific tumor suppressor. We sought to comprehensively probe the expression patterns of the gene in human normal and malignant tissues. We found that *GPRC5A* was largely expressed in normal lung and airway tissues relative to other organ-specific tissues and was consistently (across all datasets examined) suppressed in LUADs. We further studied the expression of *GPRC5A* in a dataset that we previously reported and that constituted lung tumors and normal-appearing airway cells in the adjacent cancerization field³¹. This analysis demonstrated that *GPRC5A* is down-regulated in both LUADs and the surrounding normal-appearing airway field of cancerization relative to distant normal lung tissues. It is worthwhile to mention that the expression patterns of *GPRC5A* in premalignant precursors (e.g. atypical adenomatous hyperplasia/AAH) to LUAD development is not

known. Due to the paucity of profiled AAH lesions we could not probe *GPRC5A* expression in premalignant phases of LUAD development. Analysis of *GPRC5A* expression in human lesions (AAH) that are precursors to LUAD development would shed light on the implication of this gene in the early pathogenesis of human LUAD. Of note, we previously reported that GPRC5A protein was significantly down-regulated in normal-appearing airways of lung cancer-free smokers relative to phenotypically healthy smokers³⁰. Our data suggest that *GPRC5A* exhibits an expression profile typical of an airway lineage-specific suppressor³³. These findings suggest that *Gprc5a*, a plausible airway lineage-specific gene may be suppressed in early (“normal”) phases of lung oncogenesis.

The nicotine-specific nitrosamine ketone NNK is present in tobacco and found to be causally linked to lung cancer in human smokers³⁴, suggesting that NNK exposure is a viable experimental method to mimic carcinogenic effects of cigarette smoking^{35,36}. We previously showed that *Gprc5a*^{-/-} mice developed late onset LUADs even after a single dose of the tobacco carcinogen NNK (104 mg/kg body weight)²². In order to emulate smoking-associated lung cancer in humans -- particularly in light of the fact that the majority of diagnosed lung cancers such as LUADs occur in lifetime smokers^{3,4} -- we determined to better delineate tobacco carcinogen-mediated LUAD development in *Gprc5a*^{-/-} mice, through relatively more chronic NNK exposure. Indeed, we found that this more chronic exposure (50 mg/kg per body weight three times per week for eight weeks) markedly accelerated LUAD development. Despite the fact that the *Gprc5a*^{-/-} mice are of the C57BL/6 × sv129 strain resistant to lung tumorigenesis by carcinogens such as NNK^{35,36}, all mice developed LUADs by six months following NNK exposure. It is reasonable to surmise that knockout of *Gprc5a* in the airway may render the lung more susceptible to tumorigenesis by tobacco carcinogen. It is worthwhile to mention that histopathological analysis revealed the malignant features of the LUADs exemplified by high nuclear crowding and cytological atypia²⁴ and demonstrated that the lesions comprised a mixed papillary/solid histology. Of note, this histopathological pattern is commonly observed in human LUADs³⁷ and further augments the suggestion of this model and our findings as motivation for interrogating these molecular alterations as targets for personalized prevention. More generally, our data suggest that the tobacco carcinogen-exposed *Gprc5a*^{-/-} may be a viable model to understand numerous aspects of human LUAD development in smokers.

The cell-of-origin of *Kras* mutant LUADs is still not well established. Studies in mice demonstrated that *Kras*-mutant LUADs can develop from stem cells within the bronchioalveolar junction³⁸ or from multiple cell lineages (Sftpc-expressing AT2 cells or Ccsp-positive clara cells)³⁹. In our study interrogating tobacco carcinogen-exposed *Gprc5a*^{-/-} mice, we found lesions lacked Ccsp and exclusively expressed Sftpc suggesting that they developed from AT2 cells. Our observations are in accordance with recent reports interrogating *in vivo* the cell-of-origin of LUADs. A study by Mainardi and colleagues revealed that malignant adenocarcinoma only progressed from Sftpc-expressing alveolar hyperplasias in mice engineered to express mutant *Kras* (G12V)⁴⁰. Moreover, AT2 cells were found to act as alveolar progenitor/stem cells leading to clonal foci of lesions and, subsequently, to adenocarcinomas⁴¹. Interestingly, we noted in WT normal lung tissues that expression of Gprc5a protein itself was restricted to AT1 cells. These observations are in accordance with the report by Treutlein and colleagues⁴² demonstrating, via single-cell

RNA-sequencing of mouse lung tissues, that *Gprc5a* mRNA was highly correlated with expression of *Pdpr* and with dynamic generation of AT1 cells from bipotent progenitor cells (found in the supplement of the reported study). It is important to note that various injury model studies have suggested potential pathophysiological links between both alveolar cell types and self-renewal signaling cues in AT2 cells. Earlier pneumonectomy experiments demonstrated that most AT2 cells possess latent regenerative capacity⁴³. Also, AT2 cell ablation was found to induce self-renewal (duplication) of remaining AT2 cells⁴⁴. The recent report by Desai and colleagues further demonstrated that injury (by increased oxygen tension) to AT1 cells activated stem cell renewal properties in AT2 cells and mutations of *Kras* in the latter drove constitutive self-renewal and subsequent oncogenesis⁴¹. It is reasonable to speculate that *Gprc5a* knockout may induce “molecular injury” to AT1 cells resulting in self-duplication of AT2 cells which in turn is further exacerbated by tobacco carcinogen exposure (and *Kras* mutations). Additional studies are warranted to support this plausible supposition.

Our WES analysis demonstrated that *Gprc5a*^{-/-} LUADs from NNK-treated mice overall exhibited increased total somatic mutation burdens compared to spontaneous LUADs. These data suggest that tobacco carcinogen exposure induces mutational signatures that may be involved in accelerated LUAD development. These findings are in accordance with the report by Westcott and colleagues demonstrating increased mutation burdens in tumors from mice exposed to various carcinogens (e.g. urethane) relative to tumors arising spontaneously from genetically engineered *Kras* mutant mice²⁵. Notably, our WES analysis revealed that all seven *Gprc5a*^{-/-} LUADs exhibited somatic activation mutations in *Kras* despite normal lungs from the mice being WT for the oncogene. These observed mutations (p.G12D and p.Q61R) are the same variants thought to act as drivers of human LUAD in smokers³. Our analysis of human LUADs (TCGA dataset) showed that there were no significant differences in *GPRC5A* expression based on the type of *Kras* codon 12 variant (i.e., p.G12A/C/D/V). It cannot be neglected that it is difficult to determine the natural order and causal relationship between *GPRC5A* suppression and *KRAS* (p.G12D) mutation in human LUADs that had already developed. Of note, one NNK-exposed LUAD, unlike the other four similar carcinogen derived tumors, exhibited a low somatic mutational burden concomitant with a mutation in p.Q61R. It is reasonable to speculate that different *Kras* variants may be implicated in disparate levels of mutational heterogeneity, a supposition that indeed has been previously interrogated²⁵. Further analysis in our study revealed additional (besides *Kras*) mutated *driver*²⁷ genes in *Gprc5a*^{-/-} LUADs from NNK-treated mice and in at least one of these LUADs. In contrast very few, if any, additional driver genes were mutated in the two spontaneous (from saline treated mice) LUADs. It cannot be neglected that we studied very few spontaneous/latent *Gprc5a*^{-/-} LUADs, largely due to the long latency of these lesions. Yet, our data in the *Gprc5a*^{-/-} carcinogen-exposed mouse are in line with previous reports surveying genomes of human smoker LUADs and underscoring the causal link of tobacco carcinogen exposure to increased mutational heterogeneity^{25, 26}.

Our whole-exome sequencing analysis revealed additional co-occurring mutated driver genes in the tobacco carcinogen-exposed LUADs, such as *Trp53*, *Kmt2d*, *Nf1* and *Kmt2c*. We also noted amplification of the *Ezh2* oncogene in the LUADs. Our findings in the tobacco carcinogen-exposed *Gprc5a*-knockout mouse are in close concordance with

previously reported alterations in human LUADs. In agreement with previous studies of human *Kras* mutant LUAD⁴⁵, it is also plausible that the mutated (e.g. *Trp53* and *Mll2/Kmt2d*) and copy number altered (e.g. *Ezh2* gain) driver genes that we accentuate here may cooperate with *Kras* to accelerate LUAD development in the tobacco carcinogen-exposed *Gprc5a*^{-/-} mouse. Nonetheless, particularly in light of the fact that therapies targeting *Kras* have been challenging¹³, the co-occurring mutations and CNVs described here may constitute viable targets for early treatment and prevention of *Kras* mutant LUAD. It is noteworthy, that we found various co-occurring mutated or copy number altered genes that are epigenetic regulators (e.g. *Kmt2d*, *Kmt2c* and *Ezh2*) suggesting that epigenetic deregulation may be an important mechanism in development and progression of smoke-associated *Kras* mutant LUAD. It is plausible that drugs that reprogram the epigenome (e.g. histone deacetylase and DNA methyltransferase inhibitors) may be viable agents, alone or in combination, for (chemo)prevention of this malignancy.

In conclusion, we demonstrate that *GPRC5A* is predominantly expressed in the human lung and is commonly suppressed in human LUADs. We find that relatively chronic NNK tobacco carcinogen treatment accelerates LUAD development in *Gprc5a*^{-/-} mice that otherwise develop late onset spontaneous tumors. Following WES analysis, we report that *Gprc5a*^{-/-} LUADs display activating mutations in the *Kras* oncogene. Our sequencing analysis also underscores co-occurring mutations and CNVs in additional driver genes that may cooperate with *Kras* in LUAD pathogenesis. Lastly, our findings insinuate that the tobacco carcinogen exposed *Gprc5a*^{-/-} model recapitulates carcinogen-induced *Kras* mutant LUAD; this offers a unique opportunity to map the temporal evolution of this malignancy.

Supplementary Material

Refer to Web version on PubMed Central for supplementary material.

Acknowledgments

Grant support: Supported by the University Cancer Foundation via the Institutional Research Grant program at MD Anderson Cancer Center (to H.K.), the Lung Cancer Discovery Award from the American Lung Association (to H.K.), National Cancer Institute (NCI) grant 1R01CA205608-01A1 (to P.S. and H.K.) and by NCI cancer center support grant CA16672. D.E. was supported by the Medical Research Volunteer Program (MRVP) at the American University of Beirut.

References

1. Siegel RL, Miller KD, Jemal A. Cancer Statistics, 2017. *CA: a cancer journal for clinicians*. 2017; 67:7–30. [PubMed: 28055103]
2. Torre LA, Siegel RL, Ward EM, Jemal A. Global Cancer Incidence and Mortality Rates and Trends--An Update. *Cancer epidemiology, biomarkers & prevention : a publication of the American Association for Cancer Research, cosponsored by the American Society of Preventive Oncology*. 2016; 25:16–27.
3. Herbst RS, Heymach JV, Lippman SM. Lung cancer. *N Engl J Med*. 2008; 359:1367–80. [PubMed: 18815398]
4. Kadara H, Scheet P, Wistuba II, Spira AE. Early Events in the Molecular Pathogenesis of Lung Cancer. *Cancer Prev Res (Phila)*. 2016; 9:518–27. [PubMed: 27006378]

5. Spira A, Beane J, Shah V, Liu G, Schembri F, Yang X, Palma J, Brody JS. Effects of cigarette smoke on the human airway epithelial cell transcriptome. *Proc Natl Acad Sci U S A*. 2004; 101:10143–8. [PubMed: 15210990]
6. Steiling K, Ryan J, Brody JS, Spira A. The field of tissue injury in the lung and airway. *Cancer Prev Res (Phila Pa)*. 2008; 1:396–403.
7. Cancer Genome Atlas Research N. Comprehensive molecular profiling of lung adenocarcinoma. *Nature*. 2014; 511:543–50. [PubMed: 25079552]
8. Govindan R, Ding L, Griffith M, Subramanian J, Dees ND, Kanchi KL, Maher CA, Fulton R, Fulton L, Wallis J, Chen K, Walker J, et al. Genomic landscape of non-small cell lung cancer in smokers and never-smokers. *Cell*. 2012; 150:1121–34. [PubMed: 22980976]
9. Kadara H, Choi M, Zhang J, Parra ER, Rodriguez-Canales J, Gaffney SG, Zhao Z, Behrens C, Fujimoto J, Chow C, Yoo Y, Kalthor N, et al. Whole-exome sequencing and immune profiling of early-stage lung adenocarcinoma with fully annotated clinical follow-up. *Annals of oncology : official journal of the European Society for Medical Oncology*. 2016
10. Shi J, Hua X, Zhu B, Ravichandran S, Wang M, Nguyen C, Brodie SA, Palleschi A, Alloisio M, Pariscenti G, Jones K, Zhou W, et al. Somatic Genomics and Clinical Features of Lung Adenocarcinoma: A Retrospective Study. *PLoS medicine*. 2016; 13:e1002162. [PubMed: 27923066]
11. Goldstraw P, Ball D, Jett JR, Le Chevalier T, Lim E, Nicholson AG, Shepherd FA. Non-small-cell lung cancer. *Lancet*. 2011; 378:1727–40. [PubMed: 21565398]
12. Kadota K, Sima CS, Arcila ME, Hedvat C, Kris MG, Jones DR, Adusumilli PS, Travis WD. KRAS Mutation Is a Significant Prognostic Factor in Early-stage Lung Adenocarcinoma. *The American journal of surgical pathology*. 2016; 40:1579–90. [PubMed: 27740967]
13. Tomasini P, Walia P, Labbe C, Jao K, Leigh NB. Targeting the KRAS Pathway in Non-Small Cell Lung Cancer. *The oncologist*. 2016; 21:1450–60. [PubMed: 27807303]
14. Gontan C, de Munck A, Vermeij M, Grosveld F, Tibboel D, Rottier R. Sox2 is important for two crucial processes in lung development: branching morphogenesis and epithelial cell differentiation. *Dev Biol*. 2008; 317:296–309. [PubMed: 18374910]
15. Kadara H, Wistuba II. Field cancerization in non-small cell lung cancer: implications in disease pathogenesis. *Proceedings of the American Thoracic Society*. 2012; 9:38–42. [PubMed: 22550239]
16. Bass AJ, Watanabe H, Mermel CH, Yu S, Perner S, Verhaak RG, Kim SY, Wardwell L, Tamayo P, Gat-Viks I, Ramos AH, Woo MS, et al. SOX2 is an amplified lineage-survival oncogene in lung and esophageal squamous cell carcinomas. *Nature genetics*. 2009; 41:1238–42. [PubMed: 19801978]
17. Yuan P, Kadara H, Behrens C, Tang X, Woods D, Solis LM, Huang J, Spinola M, Dong W, Yin G, Fujimoto J, Kim E, et al. Sex determining region Y-Box 2 (SOX2) is a potential cell-lineage gene highly expressed in the pathogenesis of squamous cell carcinomas of the lung. *PloS one*. 2010; 5:e9112. [PubMed: 20161759]
18. Yuan B, Li C, Kimura S, Engelhardt RT, Smith BR, Minoo P. Inhibition of distal lung morphogenesis in Nkx2.1(-/-) embryos. *Developmental dynamics : an official publication of the American Association of Anatomists*. 2000; 217:180–90. [PubMed: 10706142]
19. Weir BA, Woo MS, Getz G, Perner S, Ding L, Beroukhim R, Lin WM, Province MA, Kraja A, Johnson LA, Shah K, Sato M, et al. Characterizing the cancer genome in lung adenocarcinoma. *Nature*. 2007; 450:893–8. [PubMed: 17982442]
20. Tanaka H, Yanagisawa K, Shinjo K, Taguchi A, Maeno K, Tomida S, Shimada Y, Osada H, Kosaka T, Matsubara H, Mitsudomi T, Sekido Y, et al. Lineage-specific dependency of lung adenocarcinomas on the lung development regulator TTF-1. *Cancer Res*. 2007; 67:6007–11. [PubMed: 17616654]
21. Cheng Y, Lotan R. Molecular cloning and characterization of a novel retinoic acid-inducible gene that encodes a putative G protein-coupled receptor. *The Journal of biological chemistry*. 1998; 273:35008–15. [PubMed: 9857033]

22. Fujimoto J, Kadara H, Men T, van Pelt C, Lotan D, Lotan R. Comparative functional genomics analysis of NNK tobacco-carcinogen induced lung adenocarcinoma development in Gprc5a-knockout mice. *PLoS one*. 2010; 5:e11847. [PubMed: 20686609]
23. Tao Q, Fujimoto J, Men T, Ye X, Deng J, Lacroix L, Clifford JL, Mao L, Van Pelt CS, Lee JJ, Lotan D, Lotan R. Identification of the retinoic acid-inducible Gprc5a as a new lung tumor suppressor gene. *J Natl Cancer Inst*. 2007; 99:1668–82. [PubMed: 18000218]
24. Nikitin AY, Alcaraz A, Anver MR, Bronson RT, Cardiff RD, Dixon D, Fraire AE, Gabrielson EW, Gunning WT, Haines DC, Kaufman MH, Linnoila RI, et al. Classification of proliferative pulmonary lesions of the mouse: recommendations of the mouse models of human cancers consortium. *Cancer Res*. 2004; 64:2307–16. [PubMed: 15059877]
25. Westcott PM, Halliwill KD, To MD, Rashid M, Rust AG, Keane TM, Delrosario R, Jen KY, Gurley KE, Kemp CJ, Fredlund E, Quigley DA, et al. The mutational landscapes of genetic and chemical models of Kras-driven lung cancer. *Nature*. 2015; 517:489–92. [PubMed: 25363767]
26. Lawrence MS, Stojanov P, Polak P, Kryukov GV, Cibulskis K, Sivachenko A, Carter SL, Stewart C, Mermel CH, Roberts SA, Kiezun A, Hammerman PS, et al. Mutational heterogeneity in cancer and the search for new cancer-associated genes. *Nature*. 2013; 499:214–8. [PubMed: 23770567]
27. Vogelstein B, Papadopoulos N, Velculescu VE, Zhou S, Diaz LA Jr, Kinzler KW. Cancer genome landscapes. *Science*. 2013; 339:1546–58. [PubMed: 23539594]
28. Boeva V, Zinovyev A, Bleakley K, Vert JP, Janoueix-Lerosey I, Delattre O, Barillot E. Control-free calling of copy number alterations in deep-sequencing data using GC-content normalization. *Bioinformatics*. 2011; 27:268–9. [PubMed: 21081509]
29. Favero F, Joshi T, Marquard AM, Birkbak NJ, Krzystanek M, Li Q, Szallasi Z, Eklund AC. Sequenza: allele-specific copy number and mutation profiles from tumor sequencing data. *Annals of oncology : official journal of the European Society for Medical Oncology*. 2015; 26:64–70. [PubMed: 25319062]
30. Fujimoto J, Kadara H, Garcia MM, Kabbout M, Behrens C, Liu DD, Lee JJ, Solis LM, Kim ES, Kalhor N, Moran C, Sharafkhaneh A, et al. G-protein coupled receptor family C, group 5, member A (GPC5A) expression is decreased in the adjacent field and normal bronchial epithelia of patients with chronic obstructive pulmonary disease and non-small-cell lung cancer. *Journal of thoracic oncology : official publication of the International Association for the Study of Lung Cancer*. 2012; 7:1747–54.
31. Kadara H, Fujimoto J, Yoo SY, Maki Y, Gower AC, Kabbout M, Garcia MM, Chow CW, Chu Z, Mendoza G, Shen L, Kalhor N, et al. Transcriptomic architecture of the adjacent airway field cancerization in non-small cell lung cancer. *J Natl Cancer Inst*. 2014; 106:dju004. [PubMed: 24563515]
32. Johnson L, Mercer K, Greenbaum D, Bronson RT, Crowley D, Tuveson DA, Jacks T. Somatic activation of the K-ras oncogene causes early onset lung cancer in mice. *Nature*. 2001; 410:1111–6. [PubMed: 11323676]
33. Perdomo C, Campbell JD, Gerrein J, Tellez CS, Garrison CB, Walser TC, Drizik E, Si H, Gower AC, Vick J, Anderlind C, Jackson GR, et al. MicroRNA 4423 is a primate-specific regulator of airway epithelial cell differentiation and lung carcinogenesis. *Proc Natl Acad Sci U S A*. 2013; 110:18946–51. [PubMed: 24158479]
34. Hecht SS. Approaches to chemoprevention of lung cancer based on carcinogens in tobacco smoke. *Environmental health perspectives*. 1997; 105(4):955–63. [PubMed: 9255587]
35. Hollander MC, Balogh AR, Liwanag J, Han W, Linnoila RI, Anver MR, Dennis PA. Strain-specific spontaneous and NNK-mediated tumorigenesis in Pten^{+/-} mice. *Neoplasia*. 2008; 10:866–72. [PubMed: 18683321]
36. Zheng HC, Takano Y. NNK-Induced Lung Tumors: A Review of Animal Model. *Journal of oncology*. 2011; 2011:635379. [PubMed: 21559252]
37. Solis LM, Behrens C, Raso MG, Lin HY, Kadara H, Yuan P, Galindo H, Tang X, Lee JJ, Kalhor N, Wistuba II, Moran CA. Histologic patterns and molecular characteristics of lung adenocarcinoma associated with clinical outcome. *Cancer*. 2012; 118:2889–99. [PubMed: 22020674]

38. Kim CF, Jackson EL, Woolfenden AE, Lawrence S, Babar I, Vogel S, Crowley D, Bronson RT, Jacks T. Identification of bronchioalveolar stem cells in normal lung and lung cancer. *Cell*. 2005; 121:823–35. [PubMed: 15960971]
39. Sutherland KD, Song JY, Kwon MC, Proost N, Zevenhoven J, Berns A. Multiple cells-of-origin of mutant K-Ras-induced mouse lung adenocarcinoma. *Proc Natl Acad Sci U S A*. 2014; 111:4952–7. [PubMed: 24586047]
40. Mainardi S, Mijimolle N, Francoz S, Vicente-Duenas C, Sanchez-Garcia I, Barbacid M. Identification of cancer initiating cells in K-Ras driven lung adenocarcinoma. *Proc Natl Acad Sci U S A*. 2014; 111:255–60. [PubMed: 24367082]
41. Desai TJ, Brownfield DG, Krasnow MA. Alveolar progenitor and stem cells in lung development, renewal and cancer. *Nature*. 2014; 507:190–4. [PubMed: 24499815]
42. Treutlein B, Brownfield DG, Wu AR, Neff NF, Mantalas GL, Espinoza FH, Desai TJ, Krasnow MA, Quake SR. Reconstructing lineage hierarchies of the distal lung epithelium using single-cell RNA-seq. *Nature*. 2014; 509:371–5. [PubMed: 24739965]
43. Brody JS, Burki R, Kaplan N. Deoxyribonucleic acid synthesis in lung cells during compensatory lung growth after pneumonectomy. *The American review of respiratory disease*. 1978; 117:307–16. [PubMed: 637412]
44. Barkauskas CE, Cronce MJ, Rackley CR, Bowie EJ, Keene DR, Stripp BR, Randell SH, Noble PW, Hogan BL. Type 2 alveolar cells are stem cells in adult lung. *J Clin Invest*. 2013; 123:3025–36. [PubMed: 23921127]
45. Skoulidis F, Byers LA, Diao L, Papadimitrakopoulou VA, Tong P, Izzo J, Behrens C, Kadara H, Parra ER, Canales JR, Zhang J, Giri U, et al. Co-occurring genomic alterations define major subsets of KRAS-mutant lung adenocarcinoma with distinct biology, immune profiles, and therapeutic vulnerabilities. *Cancer discovery*. 2015; 5:860–77. [PubMed: 26069186]
46. Bhattacharjee A, Richards WG, Staunton J, Li C, Monti S, Vasa P, Ladd C, Beheshti J, Bueno R, Gillette M, Loda M, Weber G, et al. Classification of human lung carcinomas by mRNA expression profiling reveals distinct adenocarcinoma subclasses. *Proc Natl Acad Sci U S A*. 2001; 98:13790–5. [PubMed: 11707567]
47. Hou J, Aerts J, den Hamer B, van Ijcken W, den Bakker M, Riegman P, van der Leest C, van der Spek P, Foekens JA, Hoogsteden HC, Grosveld F, Philipsen S. Gene expression-based classification of non-small cell lung carcinomas and survival prediction. *PLoS one*. 2010; 5:e10312. [PubMed: 20421987]
48. Landi MT, Dracheva T, Rotunno M, Figueroa JD, Liu H, Dasgupta A, Mann FE, Fukuoka J, Hames M, Bergen AW, Murphy SE, Yang P, et al. Gene expression signature of cigarette smoking and its role in lung adenocarcinoma development and survival. *PLoS one*. 2008; 3:e1651. [PubMed: 18297132]
49. Okayama H, Kohno T, Ishii Y, Shimada Y, Shiraishi K, Iwakawa R, Furuta K, Tsuta K, Shibata T, Yamamoto S, Watanabe S, Sakamoto H, et al. Identification of genes upregulated in ALK-positive and EGFR/KRAS/ALK-negative lung adenocarcinomas. *Cancer Res*. 2012; 72:100–11. [PubMed: 22080568]
50. Selamat SA, Chung BS, Girard L, Zhang W, Zhang Y, Campan M, Siegmund KD, Koss MN, Hagen JA, Lam WL, Lam S, Gazdar AF, et al. Genome-scale analysis of DNA methylation in lung adenocarcinoma and integration with mRNA expression. *Genome research*. 2012; 22:1197–211. [PubMed: 22613842]
51. Su LJ, Chang CW, Wu YC, Chen KC, Lin CJ, Liang SC, Lin CH, Whang-Peng J, Hsu SL, Chen CH, Huang CY. Selection of DDX5 as a novel internal control for Q-RT-PCR from microarray data using a block bootstrap re-sampling scheme. *BMC Genomics*. 2007; 8:140. [PubMed: 17540040]
52. Wei TY, Juan CC, Hsu JY, Su LJ, Lee YC, Chou HY, Chen JM, Wu YC, Chiu SC, Hsu CP, Liu KL, Yu CT. Protein arginine methyltransferase 5 is a potential oncoprotein that upregulates G1 cyclins/cyclin-dependent kinases and the phosphoinositide 3-kinase/AKT signaling cascade. *Cancer science*. 2012; 103:1640–50. [PubMed: 22726390]
53. Kabbout M, Garcia MM, Fujimoto J, Liu DD, Woods D, Chow CW, Mendoza G, Momin AA, James BP, Solis L, Behrens C, Lee JJ, et al. ETS2 mediated tumor suppressive function and MET

oncogene inhibition in human non-small cell lung cancer. Clin Cancer Res. 2013; 19:3383–95.
[PubMed: 23659968]

Author Manuscript

Author Manuscript

Author Manuscript

Author Manuscript

Novelty And Impact

The development of *Kras*-mutant lung adenocarcinoma (LUAD), the most common molecular lung cancer subtype, is poorly understood. Using *in vivo* carcinogenesis models and whole-exome sequencing, we report that *Gprc5a*^{-/-} mice develop spontaneous LUADs with somatic driver *Kras* mutations. We also demonstrate that tobacco carcinogen-exposed *Gprc5a*^{-/-} mice exhibit accelerated development of LUADs harboring co-occurring mutations in additional *drivers* that may cooperate with *Kras* in LUAD pathogenesis and, thus, constitute targets for early treatment of *Kras*-mutant LUAD.

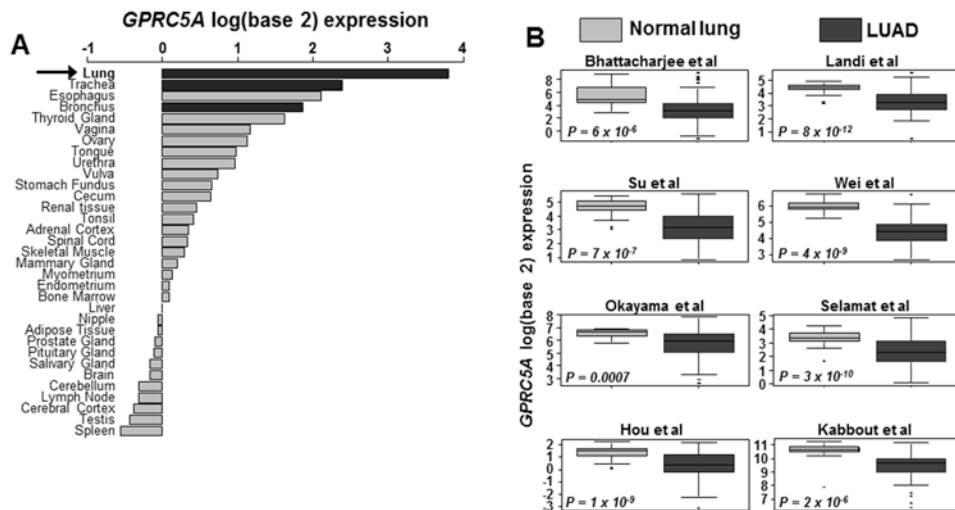


Figure 1. GPRC5A expression patterns in human normal and malignant lung tissues

A. Expression levels of *GPRC5A* mRNA were assessed in an array set comprised of human pan-normal samples (GSE7307 from the gene expression omnibus) as described in Supplementary Methods and in datasets consisting of human LUADs. Normal tissues were ranked (from top to bottom) by decreasing log (base 2) median-centered expression of *GPRC5A*. **B.** *GPRC5A* mRNA expression was also surveyed in datasets⁴⁶⁻⁵² including a set we previously reported⁵³ consisting of human LUADs and uninvolved normal tissues. Boxes represent 25% - 75% expression ranges and whiskers constitute maxima and minima. Solid horizontal lines represent median *GPRC5A* mRNA log (base 2) expression values. *P*-values were obtained using t-tests.

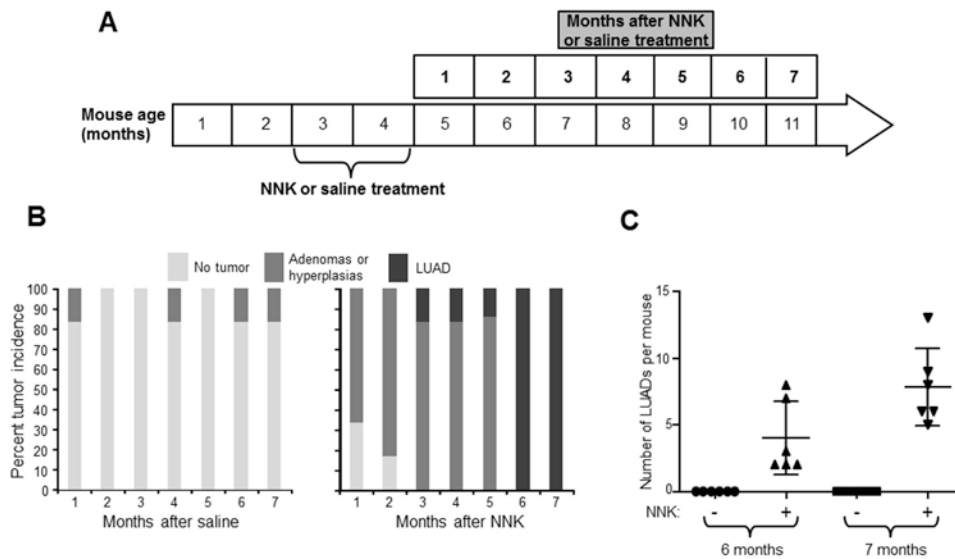


Figure 2. Tobacco carcinogen-mediated LUAD pathogenesis in the *Gprc5a*^{-/-} mouse

A. Schematic depicting timeline of NNK (three times 50mg/kg body weight per week for eight weeks) or saline treatment of eight weeks old *Gprc5a*^{-/-} mice (see Methods). Mice were divided into groups of five to six mice (per treatment and time point) and were sacrificed at every month for seven months following saline and NNK treatment. **B.** At each of the indicated time points, mice lungs were histopathologically evaluated for the development of lesions. The lesions were pathologically categorized (hyperplasias, adenomas and adenocarcinomas) based on previously reported guidelines for murine lung lesions (23) and were then enumerated and compared and contrasted across time points and between treatment groups. **C.** LUAD burdens, indicated by the number of LUADs per mouse, were statistically compared and contrasted at six and seven months following NNK treatment.

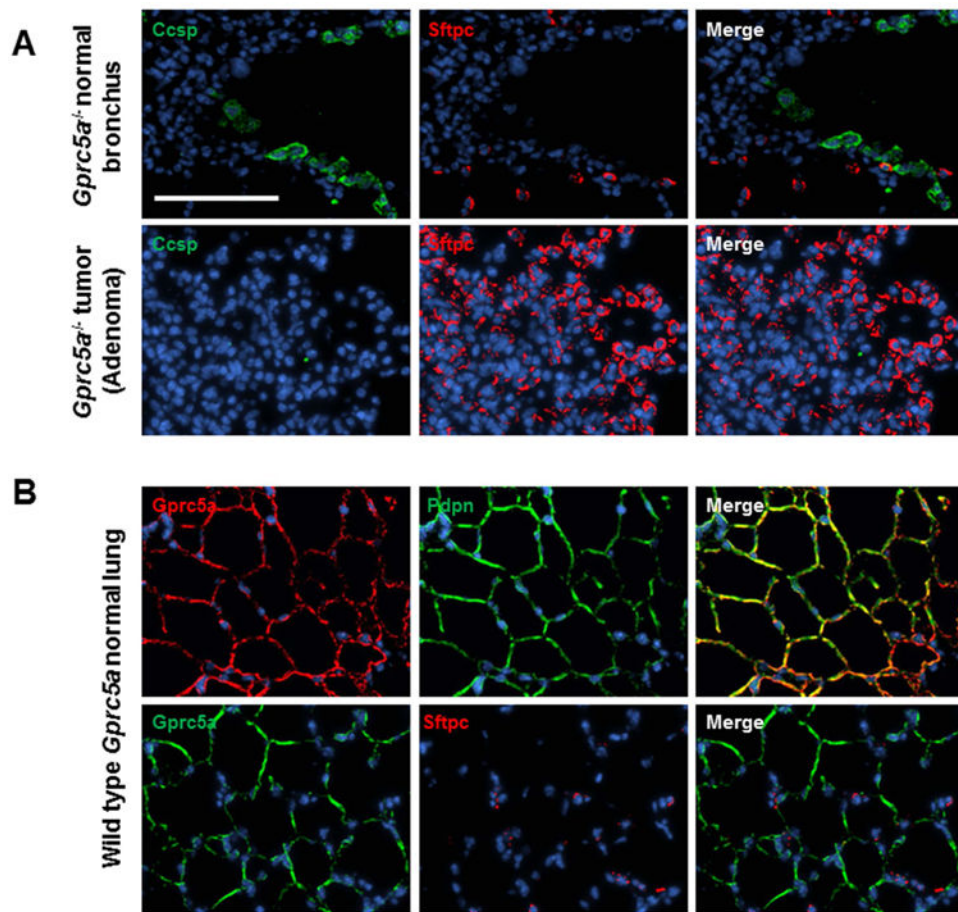


Figure 3. Immunofluorescence analysis of airway lineage markers in lung lesions and normal tissues

Immunofluorescence (IF) analysis of airway lineage markers of Clara (Ccsp) and alveolar type 2 (AT2) (Sftpc) cells was performed in *Gprc5a*^{-/-} lesions and adjacent normal regions as described in Materials and Methods. **B.** IF analysis of *Gprc5a* and the AT1 cell marker Pdpn was performed as described in Materials and Methods. All images were captured using a BX61 immunofluorescent system (Olympus) and merged using the CytoVision workstation (Leica biosystems Inc.) at a magnification of 200× (scale bar denoting 100 μm).

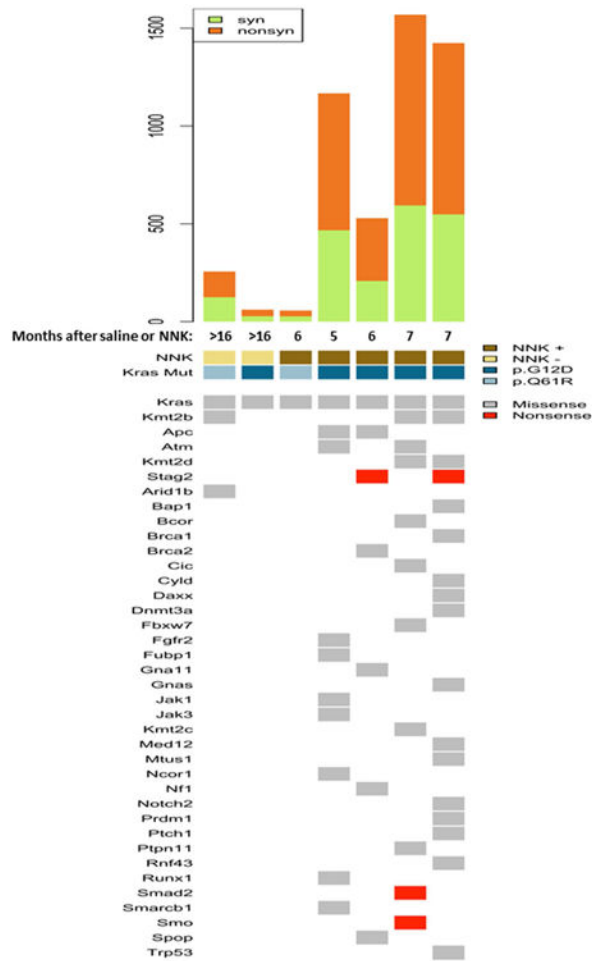


Figure 4. Whole-exome sequencing analysis of spontaneous and NNK-derived *Gprc5a*^{-/-} LUADs
 Two spontaneous (> 16 months following saline) LUADs from two *Gprc5a*^{-/-} mice as well as five LUADs that developed in different mice by five to seven months following NNK treatment were analyzed by whole-exome sequencing (WES) as described in Materials and Methods. Somatic calls were contrasted against whole-exomes from three tail veins (from two *Gprc5a*^{-/-} and one WT mice) and *Gprc5a*^{-/-} normal lung tissues at one month following saline (see Methods). Single nucleotide variants (SNVs) were prioritized based on variants occurring in *bona fide* driver genes²⁷. The top panel depicts total number of silent (syn) and non-silent (nonsyn) exonic mutations per LUAD. In the lower panel, columns represent LUADs and rows represent mutated driver genes. Arrow indicates somatic *Kras* (p.G12D or p.Q61R) mutations.

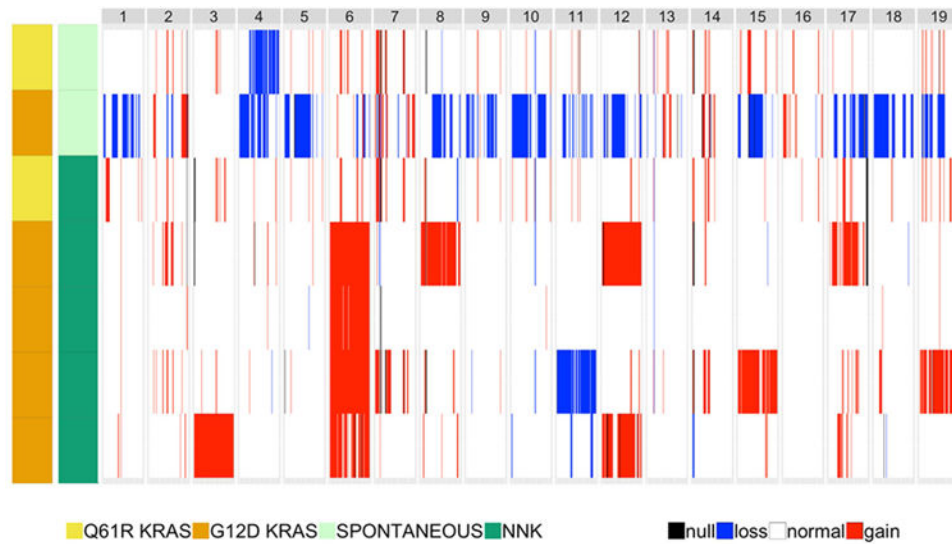


Figure 5. Genome-wide copy number variation in spontaneous and NNK-derived *Gprc5a*^{-/-} LUADs

Copy number variations (CNVs) were assessed from sequencing data and read depth using FREEC and Sequenza as described in the Supplementary Methods. Read depth was analyzed in LUADs relative to depth in normal samples to estimate copy number in 8 kb windows followed by segmentation via a LASSO-based algorithm. Genome-wide CNAs across all LUADs were then plotted. Loss, blue; gain, red; not discernable, black.